Cancer Management and Research

Dovepress

open access to scientific and medical research

Open Access Full Text Article

ORIGINAL RESEARCH

Selenium-Modified Chitosan Induces HepG2 Cell Apoptosis and Differential Protein Analysis

Su-Jun Sun[1], Peng Deng[1], Chun-E Peng[1], Hai-Yu Ji[2], Long-Fei Mao[1], Li-Zeng Peng[1]

[1]Key Laboratory of Agro-Products Processing Technology of Shandong Province, Key Laboratory of Novel Food Resources Processing Ministry of Agriculture, Institute of Agro-Food Science and Technology, Shandong Academy of Agricultural Sciences, Jinan, People's Republic of China; [2]Center for Mitochondria and Healthy Aging, College of Life Sciences, Yantai University, Yantai, People's Republic of China

Correspondence: Li-Zeng Peng, Tel +86-159-5412-8918, Email penglizeng@sdnu.edu.cn

Introduction: Chitosan is the product of the natural polysaccharide chitin removing part of the acetyl group, and exhibits various physiological and bioactive functions. Selenium modification has been proved to further enhance the chitosan bioactivities, and has been a hot topic recently.

Methods: The present study aimed to investigate the potential inhibitory mechanism of selenium-modified chitosan (SMC) on HepG2 cells through MTT assays, morphological observation, annexin V–FITC/PI double staining, mitochondrial membrane potential determination, cell-cycle detection, Western blotting, and two-dimensional gel electrophoresis (2-DE).

Results: The results indicated that SMC can induce HepG2 cell apoptosis with the cell cycle arrested in the S and G_2/M phases and gradual disruption of mitochondrial membrane potential, reduce the expression of Bcl2, and improve the expression of Bax, cytochrome C, cleaved caspase 9, and cleaved caspase 3. Also, 2-DE results showed that tubulin α_1 B chain, myosin regulatory light chain 12A, calmodulin, UPF0568 protein chromosome 14 open reading frame 166, and the cytochrome C oxidase subunit 5B of HepG2 cells were downregulated in HepG2 cells after SMC treatment.

Discussion: These data suggested that HepG2 cells induced apoptosis after SMC treatment via blocking the cell cycle in the S and G_2 /M phases, which might be mediated through the mitochondrial apoptotic pathway. These results could be of benefit to future practical applications of SMC in the food and drug fields.

Keywords: selenium-modified chitosan, antihepatoma activity, mitochondrial apoptotic pathway, differential protein analysis

Introduction

Hepatocellular carcinoma (HCC; liver cancer) is one of the most widespread malignancies and the second–most common inducement of cancer-related deaths in the world.[1,2] Modern studies have focused on developing novel chemotherapeutics to induce cancer-cell apoptosis with few side effects.[3–5] Apoptosis, a process of self-controlling suicide death, is mainly caused by intrinsic and extrinsic mechanisms.[6,7] External pathways involve ligand binding to activate death receptors and then trigger death-inducing signaling.[8,9] Intrinsic pathways, including mitochondrial pathways, can reduce the permeability of mitochondrial membranes and release cytochrome C into cytoplasm, leading to the activation of caspase families and the occurrence of cell apoptosis.[10,11]

Selenium is an essential microelement with various biological functions in both humans and animals that has been extensively studied in clinical trials.[12–14] Relevant research suggests that an inverse relationship exists between selenium intake and cancer incidence, and selenium levels are usually lower in cancer patients.[15,16] As reported, a deficiency in selenium can cause many serious health issues, including cardiovascular diseases, immunosuppression, and certain cancers.[17,18] Organic selenium compounds combining polysaccharides and proteins have presented outstanding application prospects in synthetic organic and medicinal chemistry, and have recently gained considerable interest all over the world.[19,20]

Chitosan is a partially deacetylated product of chitin that widely exists in the cell walls of fungi and the exoskeletons of some shellfish, such as lobsters and crabs.[21] It has been extensively adopted in the pharmaceutical and biomedical

Received: 4 August 2022
Accepted: 10 November 2022
Published: 28 November 2022

fields because of its favorable biocompatibility, good bioadhesivness, and low toxicity.[22] Highly purified preparations of chitosan can activate the NOD-like receptor family and NLRP3 inflammasomes in primed mouse bone marrow–derived macrophages, which induce a robust IL1β response in mouse dendritic cells, peritoneal macrophages, and human peripheral blood mononuclear cells. Studies have found that water-soluble chitosan can significantly inhibit the growth of liver cancer cells in a dose-dependent manner.[23]

Selenium-modified chitosan (SMC) is an organic selenium compound formed by complexing chitosan and selenium, thus offering the dual functions of both. Compared to inorganic selenium, SMC has been proved to possess stronger antitumor functions and lower toxicity in cancer patients.[24,25] In our previous study, SMC with a molecular weight of approximately 4827 Da was successfully synthesized by introducing a stable selenium radical (–SeO_3−) to C6–OH, C3–OH, or–NH_2 groups, and was able to effectively induce K562 cell apoptosis in a dose- and time-dependent manner in vitro.[26] Subsequently, the antitumor mechanisms of SMC in A549 cells in vitro were investigated, and it was demonstrated that SMC induced A549 cell apoptosis via a reactive oxygen species–mediated mitochondrial apoptosis pathway, which upregulated Bax and downregulated Bcl2, promoted cytochrome C release from mitochondria to cytoplasm, and activated cleaved caspase 3.[27] Then, apoptosis in A549 cells induced by SMC via the Fas–FasL signaling pathway was confirmed by our research group, which demonstrated that SMC could trigger S- and G_2 /M-phase arrest in A549 cells via upregulating the expression levels of Fas, FasL, and Fadd, and then activating the caspase cascade.[28]

However, to our knowledge, the in vitro antitumor mechanisms and differential protein analysis of SMC in HepG2 cells (one kind of human hepatocellular carcinoma cells) has not been investigated yet. Therefore, in order to expand the spectrum of SMC-induced apoptotic cells and extend areas of SMC applications, this research evaluated the cytotoxic effects of SMC on HepG2 cells and investigated the underlying mechanisms of cell apoptosis at the DNA and protein levels, which could provide a theoretical basis for the further practical applications of SMC in the food and drug fields.

Methods

Reagents

MTT, dimethyl sulfoxide (DMSO), reactive oxygen species assay kit, annexin V–FITC/PI apoptosis detection kit, and rhodamine 123 assay kit were bought from Solarbio Science & Technology (Beijing, China). Specific β-actin, Bax, Bcl2, cytochrome C, caspase 3, and caspase 9 antibodies were obtained from Tianjin Sungene Biotech (Tianjin, China). The other relevant chemicals and solvents were of analytical grade. The HepG2 cells (human liver cancer) were bought from the Shanghai Institute of Biological Sciences of the Chinese Academy of Sciences (Shanghai, China), and RPMI 1640 culture medium was employed for cell culture and SMC application.

Preparation of SMC

SMC was synthesized as described previously, and the chemical structure and molecular weight distribution of SMC are shown in Figure 1.[27] Briefly, acetic acid solution (100 mL, 5%) was employed for 10 g chitosan dissolution, and then the chitosan supernate and SeO_2 (10:1, v/w) were mixed under vacuum at 45°C for 24 h. Finally, the SMC was obtained after dialysis (molecular weight cutoff 1000 Da) against distilled water.

MTT Assay

The inhibitory effects of SMC on HepG2 cells were detected using MTT assay. HepG2 cells (100 μL) at a concentration of 5×10^4 cells/mL were seeded in 96-well plates under 37°C with 5% CO_2 and then cocultured with SMC (25, 50, 100, 200, 400, and 800 μg/mL) for 24, 36, and 48 h. Then, 20 μL MTT solution of 50 μg/mL was added to each well and incubated for 4 h and 150 μL DMSO added to dissolve formazan.[29] The positive control was 5-Fu treatment, and the negative control was no medical treatment. Finally, optical density (OD) values were evaluated using a microplate reader (model 680, Bio-Rad, Hercules, CA, USA) at 490 nm wavelength. The inhibitory effects were calculated by the formula (1 – average absorbance/control group average absorbance) × 100%.

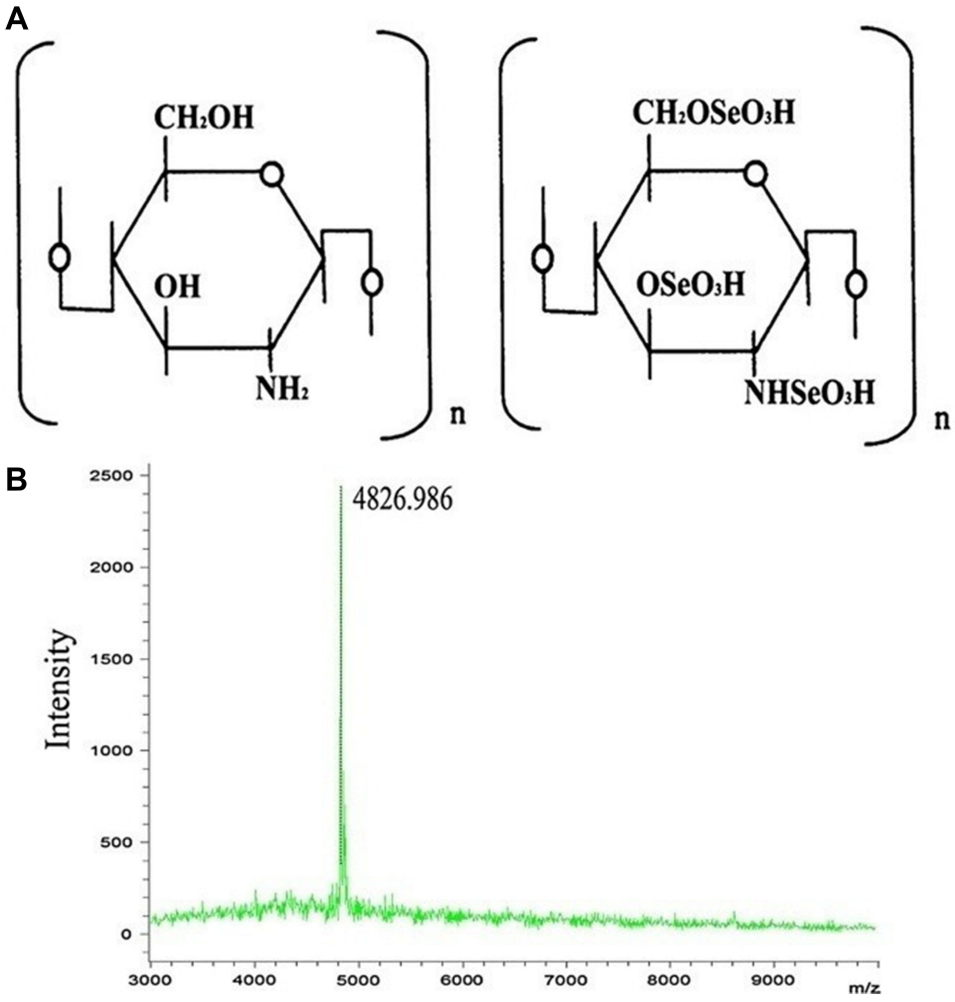

Figure 1 Chemical structure (**A**) and mass spectrum (**B**) of SMC.

Morphological Observation

HepG2 cells (3 mL) were evenly inoculated into six-well plates at a concentration of 10^5 cells/mL. After treatment with different concentrations of SMC (200 μg/mL) for 0, 24, 36, and 48 h, these HepG2 cells were photographed under an inverted optical microscope (Eclipse Ti, Nikon, Japan).[30]

Annexin V–FITC/PI Staining

HepG2 cells were harvested after incubation with SMC (200 μg/mL) for 0, 24, 36, and 48 h. Detached cells were collected by centrifugation (1000 rpm, 5 min) and attached cells by trypsinization (without EDTA). They were washed twice in PBS, resuspended in binding buffer, and adjusted to 2×10^5–5×10^5/mL. Annexin V–FITC (250 μg/mL, 5 μL) and PI (20 μg/mL, 5 μL) were added in turn, then stained for 10 min in darkness. Subsequently, the samples were processed and analyzed using flow cytometry (BD FACSCallibur, NJ, USA).

Measurement of MMP

HepG2 cells were harvested by trypsinization after incubated with SMC (200 μg/mL) for 0, 24, 36, and 48 h. They were washed (1000 rpm, 5 min) twice with PBS, and resuspended in PBS. The suspended HepG2 cells (5×10^5/mL, 1000 μL) were incubated with rhodamine 123, and the final concentration of 100 μg/mL kept at 37°C for 30 min in darkness. Finally, the stained cells were evaluated with flow cytometry (BD FACSCallibur, NJ, USA).

Cell-Cycle Analysis

Cell-cycle distributions of SMC-treated HepG2 cells were detected using PI staining. After SMC (200 μg/mL) treatments for 0, 24, 36, and 48 h, the cells were harvested and washed twice (1000 rpm, 5 min) in cold PBS, then fixed with 70% cold ethanol and stored at −20°C overnight. The fixed cells were washed twice with PBS, then incubated with RNase A (0.1 mg/mL) at 37 °C for 30 min and 50 μg/mL PI solution at 4°C for 10 min. These stained cells were measured by flow cytometry (BD FACSCallibur, NJ, USA) and the data analyzed with ModFit LT software.

Western Blot Analysis

After SMC (200 μg/mL) treatments for 0, 24, 36, and 48 h, the HepG2 cells were collected and lysed in RIPA cell-lysis buffer for 30 min and protein content determined using Coomassie blue staining. The protein samples were separated through 12% SDS-PAGE and then transferred to nitrocellulose membranes. Subsequently, these films were cut into strips according to the molecular weights of the target proteins and stained with the diluent (1:1000) Bcl2, Bax, cytochrome C, caspase 3, caspase 9, and β-actin antibodies, then horseradish peroxidase–conjugated secondary antibodies were used to incubate them for 2 h. Subsequently, an ECL-detection kit was used to assist the determination of specific protein expression on films. Finally, these films were photographed and analyzed by Quantity One software (Gel Imager; Bio-Rad, Hercules, CA, USA).

SDS-PAGE and 2-DE Analysis

The immobilized pH gradient strips (pH 3–10, linear, 11 cm, GE) were employed for further separation of total proteins in SMC-treated HepG2 cells (200 μg/mL, 36 h). The voltage settings for isoelectric focusing were 2 h at 50 V, 1 h at 100 V, 2 h at 500 V, 1 h at 1000 V, and then kept at 8000 V for 3 h. After isoelectric focusing and equilibration, the 12% SDS-PAGE gels were used to isolate these proteins based on molecular weights at 30 mA/gel for 1 h and 90 mA/gel for 2 h. Subsequently, the proteins were visualized through Coomassie brilliant blue staining and the differential proteins were identified using a MicroTOF-Q II.

Statistical Analysis

All experimental values are expressed as mean ± SD, and $p<0.05$ was considered significant using Student's *t*-test.

Results

Inhibition Effects of SMC on HepG2 Cells

The MTT assay has been widely applied in cell-viability analysis for various kinds of cells,[31] and was developed by Mossman.[32] MTT was transferred into insoluble formazan crystals after reacting with succinate dehydrogenase in mitochondria of living cells, then DMSO was employed for crystal dissolution, and these soluble liquids were detected using a microplate reader.[33] The results revealed that SMC inhibited HepG2 cell proliferation in a dose- and time-dependent manner (Figure 2). The inhibition rates of HepG2 cells significantly improved as concentrations of SMC increased from 25 μg/mL to 200 μg/mL, and then increased very gently. When the concentration of SMC was 200 μg/mL after incubation for 36 h, the cell-inhibition rate reached 81.79% and no longer continued to increase remarkably, which was similar to that of the 5-Fu group (81.25 μg/mL).

Morphological Observation

Apoptosis is an ordered geneticitally controlled process of cell death[34] that has several typical morphological features, including cell shrinkage, nuclear chromatin condensation, cytoplasmic vacuolation, plasma membrane isolation, nuclear fragmentation, and apoptotic body formation.[35] The untreated HepG2 cells appeared normal morphologically, suggesting intact membrane and regular shape. After treatment with SMC, they were shrunken with apoptotic bodies, indicating the development of apoptosis (Figure 3).

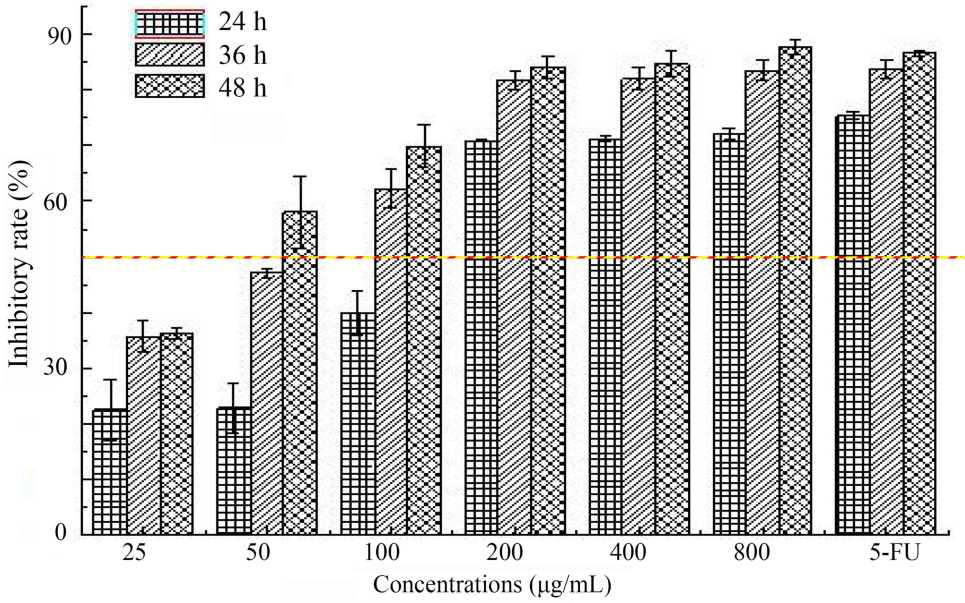

Figure 2 Inhibitory effects of SMC on HepG2 cells with different concentrations (25–800 μg/mL) and time (24 h, 36 h, 48 h).

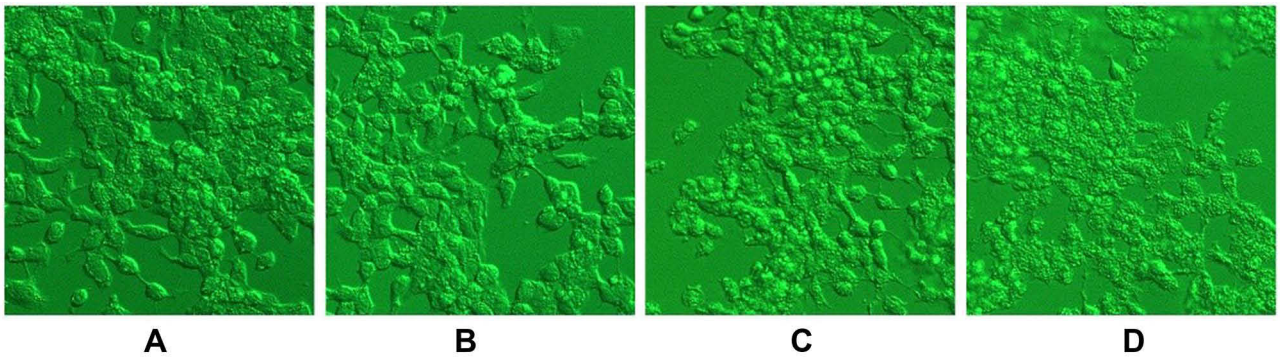

Figure 3 Morphological observation results of HepG2 cells after SMC treatments.
Notes: (**A**) 0 h, (**B**) 24 h, (**C**) 36 h, (**D**) 48 h.

Annexin V–Fluorescein Isothiocyanate/Propidium Iodide Staining

As is known to us, phosphatidylserine transfers from the inner surface of the cell membrane to the outer surface in the early stage of apoptosis and shows high affinity with annexin V. Combining fluorescently labeled annexin V with nucleic acid dye PI staining on cells distinguishes early/late apoptosis and necrosis using flow cytometry.[36,37] As shown in Figure 4, the proportions of (early apoptosis) annexin V^+–PI^- and (late apoptosis) annexin V^+–PI^+ HepG2 cells were significantly increased with the prolongation of SMC incubation. The total apoptotic rates of SMC-treated cells were increased from 1.16% to 12.33% and 63.63% and 81.00%, respectively. These results indicated that the HepG2 cells had induced apoptosis by SMC time-dependently.

Detection of Mitochondrial Membrane Potential

Rhodamine 123 was used to measure mitochondrial electric potential in intact cells by cytofluorometry. Increased fluorescence in cells reflects the electrophoretic accumulation of mitochondria.[38] As shown in Figure 5, after staining with rhodamine 12, the proportions of cells in M1 and M2 ranges represented apoptotic cells

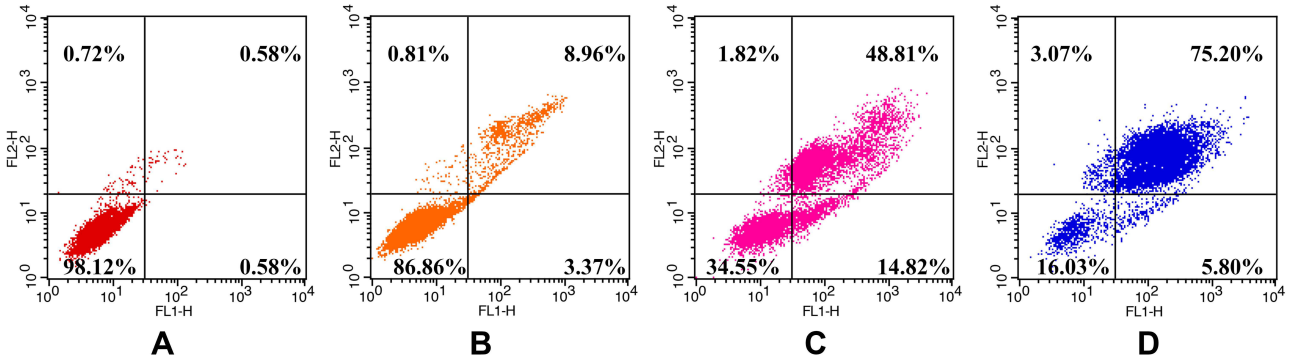

Figure 4 Apoptosis rates of HepG2 cells induced by SMC.
Notes: (**A**) 0 h, (**B**) 24 h, (**C**) 36 h, (**D**) 48 h.

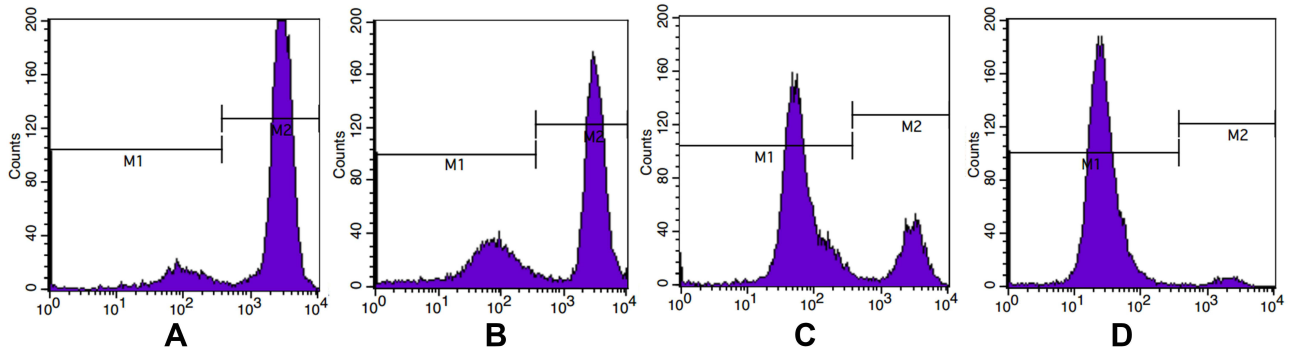

Figure 5 Effects of SMC on mitochondrial membrane potential of HepG2 cells.
Notes: (**A**) 0 h, (**B**) 24 h, (**C**) 36 h, (**D**) 48 h.

(disruption of mitochondrial membrane potential [MMP]) and normal cells, respectively. The MMP of SMC-treated HepG2 cells obviously decreased with prolongation of SMC coculture compared with the control group, which indicated that SMC induced mitochondrial dysfunction during cancer-cell apoptosis.

Cell-Cycle Distribution

PI diffuses rapidly into cells with impaired cell membranes and binds to nucleic acids after treatment with RNA enzyme, and subsequently the results of cell-cycle analysis can be obtained using flow cytometry.[39] The cell cycle of eukaryotic cells can be divided in two periods: the interphase, composed of the G_0/G_1 phase (growth preparation), S phase (synthesis of DNA), and G_2 (mitosis preparation), and the M phase (cell division), which is involved in the separation of cells' genetic materials.[40] Figure 6 shows the cell-cycle distributions of HepG2 cells after SMC treatment for 24, 36, and 48 h. The proportion of G_2/M and S phases in HepG2 cells was significantly greater than in the control group in a time-dependent fashion, while the G_0/G_1-phase cells had significantly decreased. These data suggest that HepG2 cells underwent apoptosis by S- and G_2/M-phase arrest.

Western Blotting

Western blotting analysis was conducted to determine apoptosis-related Bcl2, Bax, cytochrome C, caspase 3, and caspase 9 expression levels in HepG2 cells following SMC treatments for 0, 24, 36, or 48 h. As shown in Figure 7, a significant upregulation of Bax protein was discovered relative to the treated groups, while the expression of Bcl2 was reduced. A conspicuous accumulation in cytochrome C was detected with the increase in time, consistent with the disruption of ΔΨm (Figure 7). Subsequently, compared with untreated HepG2 cells, the expression of caspase 3 and caspase 9 gradually improved time-dependently in the SMC-treated groups. These results suggested that the

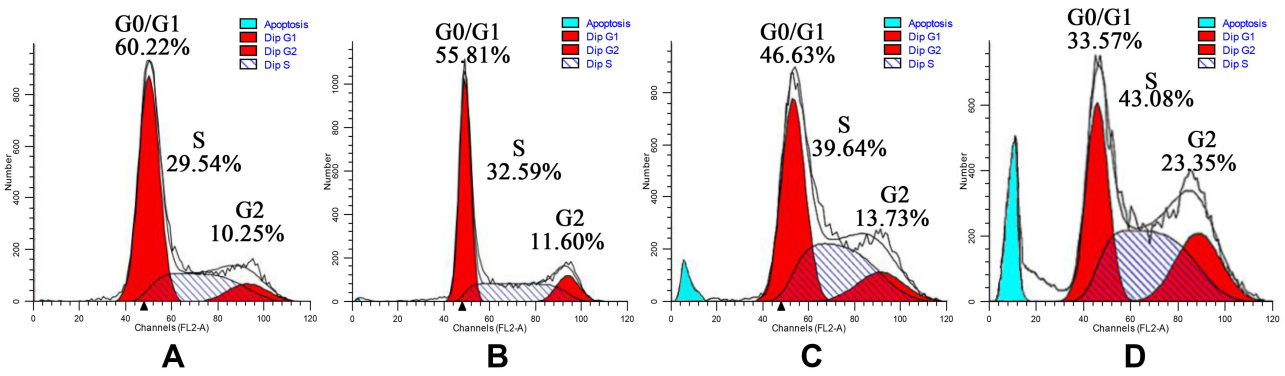

Figure 6 Effects of SMC on HepG2 cell-cycle distribution at 0 (**A**), 24 (**B**), 36 (**C**), and 48 (**D**) h.

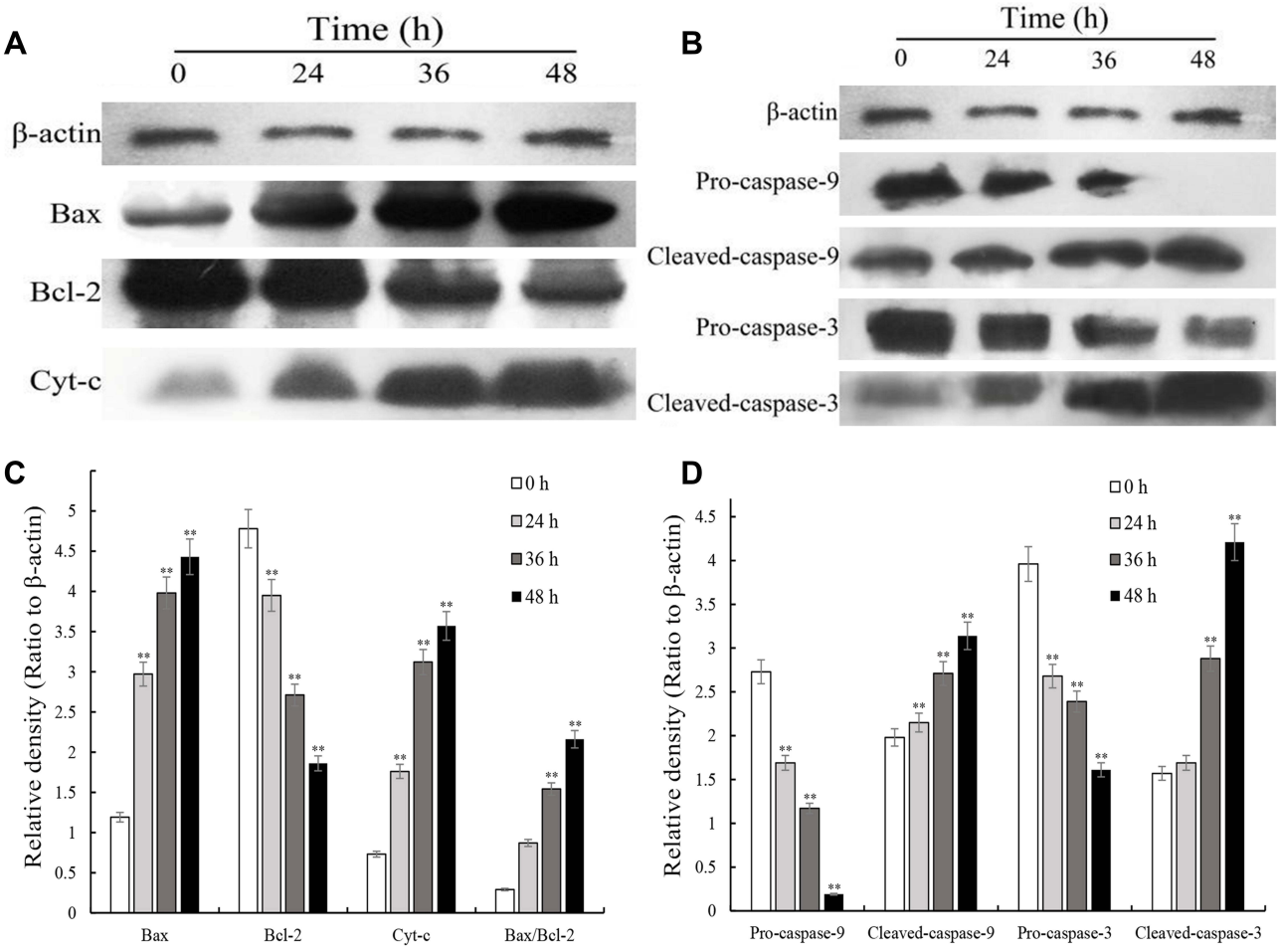

Figure 7 Expression of apoptosis-related proteins in HepG2 cells exposed to SMC for 0, 24, 36, and 48 h measured by Western blotting. (**A**) Expressions levels of β-actin, Bax, Bcl2 and CytC; (**B**) expression ratios of Bax, Bcl2, and CytC to β-actin and Bax/Bcl2; (**C**) expression levels of β-actin, pro/cleaved caspase 9 and pro/cleaved caspase 3; (**D**) expression ratios of pro/cleaved caspase 9 and pro/cleaved caspase 3 to β-actin.
Note: $^{**}p<0.01$ compared with untreated cells.

cell-apoptosis mechanism in SMC-treated HepG2 cells was mainly connected with the mitochondrial pathway by changing the expression levels of Bcl2 and Bax and reducing the MMP, which led to the release of cytochrome C and the increase in cleaved caspase 3 and cleaved caspase 9.

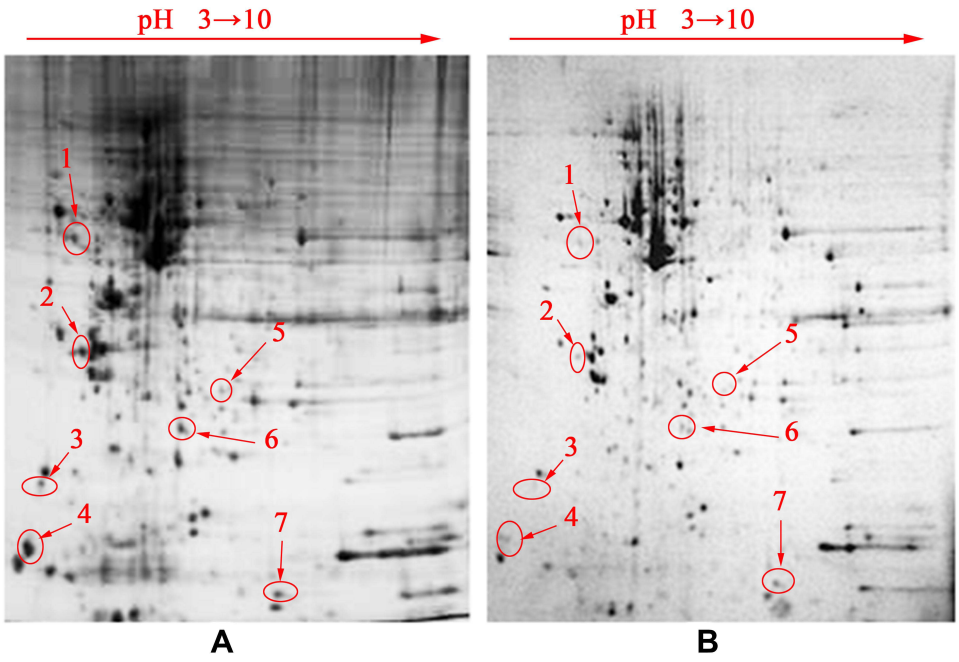

Figure 8 2-DE results of HepG2 cells from the control group (**A**) and SMC groups (**B**).
Notes: The numerals 1–7 represent the seven differential proteins detected in this experiment.

Two-Dimensional Electrophoresis

Whole-protein maps using immobilized pH gradient strips (13 cm, pH 3–10) were established by 2-DE and analysed by PD Quest to identify the differential proteins with obvious changes. As shown in Figure 8, there were 14 differential proteins selected for further identification, and the results of numbers 1, 3, 4, 6, and 7 were consistent with their isoelectric points and molecular weights. The differentially expressed proteins obtained from the 2-DE gels were analyzed and identified by MALDI-TOF/TOF-MS. Finally, five protein spots (tubulin α_1 B chain, myosin regulatory light chain 12A, calmodulin, UPF0568 protein C14orf166, and cytochrome C oxidase subunit 5B) were identified and are shown in Table 1.

Discussion

Cancer cells can proliferate without limitation because of the loss of cell-cycle regulation,[41] and modern research has aimed to develop novel drugs or adjuvants for cancer treatments by inducing cell apoptosis. Mitochondria can trigger the apoptosis of tumor cells,[42] resulting in a series of apoptotic indicators appearing, including cell shrinkage and nuclear fragmentation.[43] In the present work, SMC induced HepG2 cell apoptosis by S- and G_2/M-phase arrest, leading to disruption of MMP and morphological changes.

The mitochondrial pathway, a classical apoptosis signaling pathway, is always associated with mitochondrial dysfunction and the abnormal expression of related proteins.[44,45] *BCL2*, an antideath gene, can suppress cell

Table 1 Identification of five differentially expressed proteins

	Database	Accession number	Protein	Molecular weight (Da)	Isoelectric point	Expression
1	NCBI	gi/4507729	Tubulin α_1 B chain	50,152	4.94	Decreased
3	NCBI	gi/5453740	Myosin regulatory light chain 12 A	19794	4.65	Decreased
4	NCBI	gi/5901912	Calmodulin	16,838	4.09	Decreased
6	NCBI	gi/7706322	UPF0568 protein C14orf166	28,068	6.19	Decreased
7	NCBI	gi/17017988	Cytochrome C oxidase subunit 5B	13696	9.07	Decreased

apoptosis, while Bax can induce mitochondrial function disorder, leading to the release of various cell-apoptosis mediators.[46,47] The relative expression ratio of Bax to Bcl2 is an important indicator of the state of cells.[48] Cytoplasmic cytochrome C has an apoptosis-promoting role in normal or cancer cells.[49] In this study, SMC induced MMP disruption and improved the expression of Bax while decreasing that of Bcl2, leading to cytochrome C being released into cytoplasm and contributing to triggering of the apoptosis of HepG2 cells. Cytoplasmic cytochrome C may participate in activating caspase 9 in a manner dependent on adenosine triphosphate.[50] Subsequently, the active caspase 9 is expected to cleave caspase 3 and PARP[51] and induce cell apoptosis via the mitochondrial signal pathway.[52,53] In this study, the expression levels of cleaved caspase 9 and cleaved caspase 3 in SMC-treated HepG2 cells were obviously higher after activation by cytochrome C in cytoplasm, thereby initiating the apoptosis process.

It is known that α-tubulin plays important roles in reorganizing and dissembling microtubule combinations, thereby regulating the cell life cycle and mitosis. Its decreased expression can cause proliferation inhibition or apoptosis of cells.[54] Myosin regulatory light chain 12A is the major regulatory domain in the formation process of globulin-catalyzed supramolecular complexes. Phosphorylation of myosin plays crucial roles in tumor-cell growth and invasion.[13,55] Calmodulin has become a potential target for cancer therapy.[56,57] Some drugs exhibit antitumor effects via binding to calmodulin and altering the molecular conformation, thereby inhibiting calmodulin-regulated target enzymes, such as myosin light chain kinase, affecting cell metabolism, cell growth, and other biological activities.[58] C14orf166 is an open-reading-frame sequence expressing protein products involved in the mitosis of cells and the formation of centrosome structures that is expressed in various tumor cell lines, although the mechanism of action in tumors remains unknown.[59,60] Cytochrome C oxidase is an electron-transporting, rate-limiting enzyme that catalyzes the oxidation of reduced cytochrome C. Its abnormal expression can directly affect the oxidation of cytochrome C and trigger dysfunction among mitochondria, leading to excessive ROS accumulation and abnormal cell status.[61–64] As such, the findings of lower expression levels of these proteins in SMC-treated HepG2 cells indicated that SMC effectively inhibited the proliferation of cancer cells, reduced their viability, caused mitochondrial dysfunction, and finally resulted in HepG2 cell apoptosis, which is consistent with previous results.

Conclusion

Our results demonstrated that SMC caused the mitochondrial dysfunction of HepG2 cells by arresting the cell cycle in the S and G_2/M phases and inducing apoptosis via the mitochondrial apoptotic pathway. Tubulin α_1 B chain, myosin regulatory light chain 12A, calmodulin, UPF0568 protein C14orf166, and cytochrome C oxidase subunit 5B expression levels in SMC-treated HepG2 cells all decreased, which further indicated that cell apoptosis was mediated through mitochondria. These results could provide a theoretical basis and data support for further practical applications of SMC in the food and drug fields.

Funding

This research was funded by the Agricultural Science and Technology Innovation Project (CXGC2021B18), National Natural Science Foundation of China (32101035), and the Natural Science Foundation of Shandong Province (ZR2021QC025).

Disclosure

The authors declare that they have no conflicts of interest in this work.

References

1. Aggarwal M, Arain A, Jin Z. Systemic treatment for hepatocellular carcinoma. *Chronic Dis Transl Med*. 2018;4(3):148–155. doi:10.1016/j.cdtm.2018.08.003
2. El-Senduny FF, Shabana SM, Rösel D, et al. Urea-functionalized organoselenium compounds as promising anti-HepG2 and apoptosis-inducing agents. *Future Med Chem*. 2021;13(19):1655–1677. doi:10.4155/fmc-2021-0114
3. Duan X, Gao S, Li J, et al. Acute arsenic exposure induces inflammatory responses and CD4+ T cell subpopulations differentiation in spleen and thymus with the involvement of MAPK, NF-kB, and Nrf2. *Mol Immunol*. 2017;81:160–172. doi:10.1016/j.molimm.2016.12.005

4. Singh S, Utreja D, Kumar V. Pyrrolo[2,1-f][1,2,4]triazine: a promising fused heterocycle to target kinases in cancer therapy. *Med Chem Res*. 2022;31(1):1–25. doi:10.1007/s00044-021-02819-1
5. Shaaban S, Shabana SM, Al-Faiyz YS, et al. Enhancing the chemosensitivity of HepG2 cells towards cisplatin by organoselenium pseudopeptides. *Bioorg Chem*. 2021;109:104713. doi:10.1016/j.bioorg.2021.104713
6. Jiang Y, Miao J, Wang D, et al. MAP30 promotes apoptosis of U251 and U87 cells by suppressing the LGR5 and Wnt/β-catenin signaling pathway, and enhancing Smac expression. *Oncol Lett*. 2018;15(4):5833–5840. doi:10.3892/ol.2018.8073
7. Tang C, Wang J, Wei Q, et al. Tropomyosin-1 promotes cancer cell apoptosis via the p53-mediated mitochondrial pathway in renal cell carcinoma. *Oncol Lett*. 2018;15(5):7060–7068. doi:10.3892/ol.2018.8204
8. Hancz D, Szabo A, Molnar T, et al. Flagellin increases death receptor-mediated cell death in a RIP1-dependent manner. *Immunol Lett*. 2018;193:42–50. doi:10.1016/j.imlet.2017.11.007
9. Jaeschke H, Duan L, Akakpo JY, et al. The role of apoptosis in Acetaminophen hepatotoxicity. *Food Chem Toxicol*. 2018;118:709–718. doi:10.1016/j.fct.2018.06.025
10. Kumar K, Sabarwal A, Singh RP. Mancozeb selectively induces mitochondrial-mediated apoptosis in human gastric carcinoma cells through ROS generation. *Mitochondrion*. 2019;48:1–10. doi:10.1016/j.mito.2018.06.003
11. Yu J, Dong X-D, Jiao J-S, et al. The inhibitory effects of selenium nanoparticles modified by fructose-enriched polysaccharide from Codonopsis pilosula on HepG2 cells. *Ind Crops Prod*. 2022;176:114335. doi:10.1016/j.indcrop.2021.114335
12. Estevez H, Garcia-Lidon JC, Luque-Garcia JL, et al. Effects of chitosan-stabilized selenium nanoparticles on cell proliferation, apoptosis and cell cycle pattern in HepG2 cells: comparison with other selenospecies. *Colloids Surf B Biointerfaces*. 2014;122:184–193. doi:10.1016/j.colsurfb.2014.06.062
13. Norwood Toro LE, Wang Y, Condeelis JS, et al. Myosin-IIA heavy chain phosphorylation on S1943 regulates tumor metastasis. *Exp Cell Res*. 2018;370(2):273–282. doi:10.1016/j.yexcr.2018.06.028
14. Shaaban S, Ashmawy AM, Negm A, et al. Synthesis and biochemical studies of novel organic selenides with increased selectivity for hepatocellular carcinoma and breast adenocarcinoma. *Eur J Med Chem*. 2019;179:515–526. doi:10.1016/j.ejmech.2019.06.075
15. Whanger PD. Selenium and its relationship to cancer: an update. *Br J Nutr*. 2007;91(1):11–28. doi:10.1079/BJN20031015
16. Mohamed Gouda YJA, Abd El-Lateef HM, Khalaf MM, Shaaban S. Design, synthesis, and biological evaluations of novel naphthalene-based organoselenocyanates. *Biointerface Res Appl Chem*. 2023;13(3):219.
17. Dinh QT, Cui Z, Huang J, et al. Selenium distribution in the Chinese environment and its relationship with human health: a review. *Environ Int*. 2018;112:294–309. doi:10.1016/j.envint.2017.12.035
18. Sak M, Al-Faiyz YS, Elsawy H, et al. Novel organoselenium redox modulators with potential anticancer, antimicrobial, and antioxidant activities. *Antioxidants*. 2022;11:071231. doi:10.3390/antiox11071231
19. Shaaban S, El-Lateef HMA, Khalaf MM, et al. One-pot multicomponent polymerization, metal-, and non-metal-catalyzed synthesis of organoselenium compounds. *Polymers*. 2022;14:112208. doi:10.3390/polym14112208
20. Shaaban S, Zarrouk A, Vervandier-Fasseur D, et al. Cytoprotective organoselenium compounds for oligodendrocytes. *Arab J Chem*. 2021;14(4):103051. doi:10.1016/j.arabjc.2021.103051
21. Arjunan N, Singaravelu CM, Kulanthaivel J, et al. A potential photocatalytic, antimicrobial and anticancer activity of chitosan-copper nanocomposite. *Int J Biol Macromol*. 2017;104:1774–1782. doi:10.1016/j.ijbiomac.2017.03.006
22. Kolawole OM, Lau WM, Khutoryanskiy VV. Methacrylated chitosan as a polymer with enhanced mucoadhesive properties for transmucosal drug delivery. *Int J Pharm*. 2018;550(1):123–129. doi:10.1016/j.ijpharm.2018.08.034
23. Mohammed MH, Williams PA, Tverezovskaya O. Extraction of chitin from prawn shells and conversion to low molecular mass chitosan. *Food Hydrocoll*. 2013;31(2):166–171. doi:10.1016/j.foodhyd.2012.10.021
24. Li S, Bian F, Yue L, et al. Selenium-dependent antitumor immunomodulating activity of polysaccharides from roots of A. membranaceus. *Int J Biol Macromol*. 2014;69:64–72. doi:10.1016/j.ijbiomac.2014.05.020
25. Cheng L, Chen L, Yang Q, et al. Antitumor activity of Se-containing tea polysaccharides against sarcoma 180 and comparison with regular tea polysaccharides and Se-yeast. *Int J Biol Macromol*. 2018;120:853–858. doi:10.1016/j.ijbiomac.2018.08.154
26. Liu A, Song W, Cao D, et al. Growth inhibition and apoptosis of human leukemia K562 cells induced by seleno-short-chain chitosan. *Methods Find Exp Clin Pharmacol*. 2008;30(3):181–186. doi:10.1358/mf.2008.30.3.1213209
27. Zhao Y, Zhang S, Wang P, et al. Seleno-short-chain chitosan induces apoptosis in human non-small-cell lung cancer A549 cells through ROS-mediated mitochondrial pathway. *Cytotechnology*. 2017;69(6):851–863. doi:10.1007/s10616-017-0098-z
28. Gao J, Zhao Y, Wang C, et al. A novel synthetic chitosan selenate (CS) induces apoptosis in A549 lung cancer cells via the Fas/FasL pathway. *Int J Biol Macromol*. 2020;158:689–697. doi:10.1016/j.ijbiomac.2020.05.016
29. Ji H-Y, Yu J, Jiao J-S, et al. Ultrasonic-assisted extraction of codonopsis pilosula glucofructan: optimization, structure, and immunoregulatory activity. *Nutrients*. 2022;14(5):927. doi:10.3390/nu14050927
30. Yu J, Ji H, Dong X, et al. Apoptosis of human gastric carcinoma MGC-803 cells induced by a novel Astragalus membranaceus polysaccharide via intrinsic mitochondrial pathways. *Int J Biol Macromol*. 2019;126:811–819. doi:10.1016/j.ijbiomac.2018.12.268
31. Nga NTH, Ngoc TTB, Trinh NTM, et al. Optimization and application of MTT assay in determining density of suspension cells. *Anal Biochem*. 2020;610:113937. doi:10.1016/j.ab.2020.113937
32. Mosmann T. Rapid colorimetric assay for cellular growth and survival: application to proliferation and cytotoxicity assays. *J Immunol Methods*. 1983;65(1):55–63. doi:10.1016/0022-1759(83)90303-4
33. Tada H, Shiho O, Kuroshima K-I, et al. An improved colorimetric assay for interleukin 2. *J Immunol Methods*. 1986;93(2):157–165. doi:10.1016/0022-1759(86)90183-3
34. Fesik SW. Promoting apoptosis as a strategy for cancer drug discovery. *Nat Rev Cancer*. 2005;5(11):876–885. doi:10.1038/nrc1736
35. Doonan F, Cotter TG. Morphological assessment of apoptosis. *Methods*. 2008;44(3):200–204. doi:10.1016/j.ymeth.2007.11.006
36. Sawai H, Domae N. Discrimination between primary necrosis and apoptosis by necrostatin-1 in Annexin V-positive/propidium iodide-negative cells. *Biochem Biophys Res Commun*. 2011;411(3):569–573. doi:10.1016/j.bbrc.2011.06.186
37. Perumalsamy H, Sankarapandian K, Kandaswamy N, et al. Cellular effect of styrene substituted biscoumarin caused cellular apoptosis and cell cycle arrest in human breast cancer cells. *Int J Biochem Cell Biol*. 2017;92:104–114. doi:10.1016/j.biocel.2017.09.019

38. Baracca A, Sgarbi G, Solaini G, et al. Rhodamine 123 as a probe of mitochondrial membrane potential: evaluation of proton flux through F0 during ATP synthesis. *Biochim Biophys Acta- Bioenerg*. 2003;1606(1):137–146. doi:10.1016/S0005-2728(03)00110-5
39. Happ DF, Tasker RA. A method for objectively quantifying propidium iodide exclusion in organotypic hippocampal slice cultures. *J Neurosci Methods*. 2016;269:1–5. doi:10.1016/j.jneumeth.2016.05.006
40. Leal-Esteban LC, Fajas L. Cell cycle regulators in cancer cell metabolism. *Biochim Biophys Acta-Mol Basis Dis*. 2020;1866(5):165715. doi:10.1016/j.bbadis.2020.165715
41. Wang N, Han Y, Luo L, et al. β-asarone induces cell apoptosis, inhibits cell proliferation and decreases migration and invasion of glioma cells. *Biomed Pharmacother*. 2018;106:655–664. doi:10.1016/j.biopha.2018.06.169
42. Yaacoub K, Pedeux R, Tarte K, et al. Role of the tumor microenvironment in regulating apoptosis and cancer progression. *Cancer Lett*. 2016;378(2):150–159. doi:10.1016/j.canlet.2016.05.012
43. Xie P, Horio F, Fujii I, et al. A novel polysaccharide derived from algae extract inhibits cancer progression via JNK, not via the p38 MAPK signaling pathway. *Int J Oncol*. 2018;52(5):1380–1390. doi:10.3892/ijo.2018.4297
44. Cao H, Xu H, Zhu G, et al. Isoquercetin ameliorated hypoxia/reoxygenation-induced H9C2 cardiomyocyte apoptosis via a mitochondrial-dependent pathway. *Biomed Pharmacother*. 2017;95:938–943. doi:10.1016/j.biopha.2017.08.128
45. Ya G. A Lentinus edodes polysaccharide induces mitochondrial-mediated apoptosis in human cervical carcinoma HeLa cells. *Int J Biol Macromol*. 2017;103:676–682. doi:10.1016/j.ijbiomac.2017.05.085
46. Birkinshaw RW, Czabotar PE. The BCL-2 family of proteins and mitochondrial outer membrane permeabilisation. *Semin Cell Dev Biol*. 2017;72:152–162. doi:10.1016/j.semcdb.2017.04.001
47. Fan S, Zhang J, Nie W, et al. Antitumor effects of polysaccharide from Sargassum fusiforme against human hepatocellular carcinoma HepG2 cells. *Food Chem Toxicol*. 2017;102:53–62. doi:10.1016/j.fct.2017.01.020
48. Liu W-B, Xie F, Sun H-Q, et al. Anti-tumor effect of polysaccharide from Hirsutella sinensis on human non-small cell lung cancer and nude mice through intrinsic mitochondrial pathway. *Int J Biol Macromol*. 2017;99:258–264. doi:10.1016/j.ijbiomac.2017.02.071
49. Karimi Pur MR, Hosseini M, Faridbod F, et al. Early detection of cell apoptosis by a cytochrome C label-Free electrochemiluminescence aptasensor. *Sens Actuators B Chem*. 2018;257:87–95. doi:10.1016/j.snb.2017.10.138
50. Li P, Nijhawan D, Budihardjo I, et al. Cytochrome c and dATP-dependent formation of apaf-1/caspase-9 complex initiates an apoptotic protease cascade. *Cell*. 1997;91(4):479–489. doi:10.1016/S0092-8674(00)80434-1
51. McArthur K, Kile BT. Apoptotic caspases: multiple or mistaken identities? *Trends Cell Biol*. 2018;28(6):475–493. doi:10.1016/j.tcb.2018.02.003
52. Song T, Yao Y, Wang T, et al. Tanshinone IIA ameliorates apoptosis of myocardiocytes by up-regulation of miR-133 and suppression of Caspase-9. *Eur J Pharmacol*. 2017;815:343–350. doi:10.1016/j.ejphar.2017.08.041
53. Yang Y, Zong M, Xu W, et al. Natural pyrethrins induces apoptosis in human hepatocyte cells via Bax- and Bcl-2-mediated mitochondrial pathway. *Chem Biol Interact*. 2017;262:38–45. doi:10.1016/j.cbi.2016.12.006
54. Gadau SD. Morphological and quantitative analysis on α-tubulin modifications in glioblastoma cells. *Neurosci Lett*. 2018;687:111–118. doi:10.1016/j.neulet.2018.09.044
55. Almansour K, Taverner A, Eggleston IM, et al. Mechanistic studies of a cell-permeant peptide designed to enhance myosin light chain phosphorylation in polarized intestinal epithelia. *J Control Release*. 2018;279:208–219. doi:10.1016/j.jconrel.2018.03.033
56. Berchtold MW, Villalobo A. The many faces of calmodulin in cell proliferation, programmed cell death, autophagy, and cancer. *Biochim Biophys Acta-Mol Basis Dis*. 2014;1843(2):398–435.
57. Yokokura S, Yurimoto S, Matsuoka A, et al. Calmodulin antagonists induce cell cycle arrest and apoptosis in vitro and inhibit tumor growth in vivo in human multiple myeloma. *BMC Cancer*. 2014;14(1):882. doi:10.1186/1471-2407-14-882
58. Höpker K, Hagmann H, Khurshid S, et al. AATF/Che-1 acts as a phosphorylation-dependent molecular modulator to repress p53-driven apoptosis. *EMBO J*. 2012;31(20):3961–3975. doi:10.1038/emboj.2012.236
59. Liu JY, Zhang NZ, Li WH, et al. Proteomic analysis of differentially expressed proteins in the three developmental stages of Trichinella spiralis. *Vet Parasitol*. 2016;231:32–38. doi:10.1016/j.vetpar.2016.06.021
60. Peng RY, Ren HJ, Zhang CL, et al. Comparative proteomics analysis of Trichinella spiralis muscle larvae exposed to albendazole sulfoxide stress. *Acta Trop*. 2018;185:183–192. doi:10.1016/j.actatropica.2017.12.023
61. Niu Z, Zhang W, Gu X, et al. Mitophagy inhibits proliferation by decreasing cyclooxygenase-2 (COX-2) in arsenic trioxide-treated HepG2 cells. *Environ Toxicol Pharmacol*. 2016;45:212–221. doi:10.1016/j.etap.2016.06.006
62. Liu J, Lu F, Gong Y, et al. High expression of synthesis of cytochrome c oxidase 2 and TP53-induced glycolysis and apoptosis regulator can predict poor prognosis in human lung adenocarcinoma. *Hum Pathol*. 2018;77:54–62. doi:10.1016/j.humpath.2017.12.029
63. Saxena M, Delgado Y, Sharma RK, et al. Inducing cell death in vitro in cancer cells by targeted delivery of cytochrome c via a transferrin conjugate. *PLoS One*. 2018;13(4):e0195542. doi:10.1371/journal.pone.0195542
64. Thangarajan S, Vedagiri A, Somasundaram S, et al. Neuroprotective effect of morin on lead acetate- induced apoptosis by preventing cytochrome c translocation via regulation of Bax/Bcl-2 ratio. *Neurotoxicol Teratol*. 2018;66:35–45. doi:10.1016/j.ntt.2018.01.006